Deploying Wireless Sensors to Achieve Both Coverage and Connectivity

Xiaole Bai† Santosh Kumar† Dong Xuan† Ziqiu Yun‡ Ten H. Lai†

† Computer Science and Engineering
The Ohio State University
Columbus, OH 43210, USA
{baixia,kumars,xuan,lai}@cse.ohio-state.edu

‡ Department of Mathematics
Suzhou University
Suzhou, 215006, P.R.CHINA
yunziqiu@public1.sz.js.cn

ABSTRACT

It is well-known that placing disks in the triangular lattice pattern is optimal for achieving full coverage on a plane. With the emergence of wireless sensor networks, however, it is now no longer enough to consider coverage alone when deploying a wireless sensor network; connectivity must also be considered. While moderate loss in coverage can be tolerated by applications of wireless sensor networks, loss in connectivity can be fatal. Moreover, since sensors are subject to unanticipated failures after deployment, it is not enough to have a wireless sensor network just connected, it should be k-connected (for $k > 1$). In this paper, we propose an optimal deployment pattern to achieve both full coverage and 2-connectivity, and prove its optimality for all values of r_c/r_s, where r_c is the communication radius, and r_s is the sensing radius. We also prove the optimality of a previously proposed deployment pattern for achieving both full coverage and 1-connectivity, when $r_c/r_s < \sqrt{3}$. Finally, we compare the efficiency of some popular regular deployment patterns such as the square grid and triangular lattice, in terms of the number of sensors needed to provide coverage and connectivity.

Categories and Subject Descriptors

C.2.1 [**Computer-Communication networks**]: Network Architecture and Design – *network topology*

General Terms

Theory

Keywords

Coverage, Connectivity, optimal deployment pattern.

1. INTRODUCTION

It is well-known that placing disks on the vertices of a triangular lattice (or, equivalently, at the centers of regular hexagons, as illustrated in Figure 3) is optimal, in terms of the number of disks needed to achieve *full coverage* of a plane. Its asymptotic optimality was proved rigorously in a 1939 paper [6], and was recently reproved in [9] using a different approach.

With the emergence of wireless sensor networks in the past decade, consideration of coverage alone is no longer enough when deploying sensors. The sensor network needs to be *connected* too. On the problem of achieving both coverage and connectivity at the same time, a few results are known in the literature. First, when the communication range r_c is at least twice the sensing range r_s (i.e., $r_c \geq 2r_s$), then coverage of a region implies connectivity in the sensor network [8]. Second, if $r_c \geq \sqrt{3}r_s$, then deploying sensors in the triangular lattice pattern provides both coverage and connectivity, and is optimal in terms of the number of sensors needed. Third, when $r_c = r_s$, a strip-based deployment pattern is near optimal [5]. But, no results are known for general values of r_c/r_s.

It is important, however, to investigate the optimal deployment pattern to achieve both coverage and connectivity for general values of r_c/r_s because in practice they can be any value. For example, while the reliable communication range of the Extreme Scale Mote (XSM) platform is 30 m, the sensing range of the acoustics sensor for detecting an All Terrain Vehicle is 55 m [1]. In this case, $r_c/r_s \ll \sqrt{3}$. Sometimes even when it is claimed for a sensor platform to have $r_c/r_s \geq \sqrt{3}$, it may not hold in practice because the reliable communication range is often 60-80% of the claimed value [10].

Further, we note that having a wireless sensor network just 1-connected is not much useful in practice. This is because some sensors fail right after deployment due to factors beyond human control, and more continue to fail gradually with time [2]. Moderate loss in coverage may be tolerated by applications but loss in connectivity can be fatal as it can render an entire portion of the network useless — their sensing data can not reach the base station. Therefore, it is desirable to have higher degrees of connectivity in wireless sensor networks. But, the problem of determining the optimal deployment pattern that achieves both coverage and k-connectivity for general values of k and r_c/r_s is an open problem.

1.1 Our Contributions

In this paper, we propose and prove the asymptotic optimality of a deployment pattern (shown in Figure 1) to achieve both coverage and 2-connectivity for all values of r_c/r_s.

We also extend the result of [5] and show that the strip-based deployment pattern (shown in Figure 2) is not only near-optimal but asymptotically optimal for achieving both

MobiHoc'06, May 22–25, 2006, Florence, Italy.

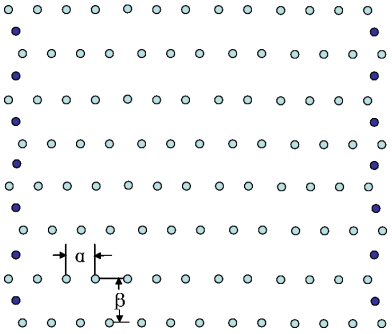

Figure 1: Strip-based deployment pattern to achieve coverage and 2-connectivity. The light-filled dots show the sensor locations that form the horizontal strip, while the dark-filled dots form the two vertical strips. Here, $\alpha = \min\{r_c, \sqrt{3}r_s\}$ and $\beta = r_s + \sqrt{r_s^2 - \alpha^2/4}$. The vertical strip of sensors may be removed when $r_c/r_s \geq \sqrt{3}$.

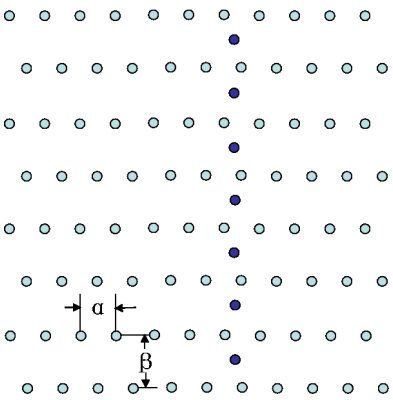

Figure 2: Strip-based deployment that is optimal for achieving coverage with 1-connectivity, when $r_c/r_s < \sqrt{3}$. The light-filled dots show the sensor locations that form the horizontal strip, while the dark-filled dots form the one vertical strip. Here, $\alpha = \min\{r_c, \sqrt{3}r_s\}$ and $\beta = r_s + \sqrt{r_s^2 - \alpha^2/4}$.

full coverage and 1-connectivity. Moreover, its optimality holds not only for $r_c/r_s = 1$ but for all $r_c/r_s < \sqrt{3}$.

In practice, wireless sensor networks are often desired to follow regular patterns due to at least two reasons — 1) convenience of deployment and 2) to achieve a higher degree of connectivity. Four popular regular deployment patterns are hexagon, square grid, rhombus, and equilateral triangle, all of which are exhibited in Figure 3. Note that the triangular lattice pattern provides at least 6-connectivity, square grid provides at least 4-connectivity, rhombus provides at least 4 or 6 connectivity depending on its shape, and the hexagon provides at least 3-connectivity[1]. Connectivity aside, it would be interesting to know: (1) which of these four regular patterns is more efficient than the others (in terms of the number of sensors needed)? (2) what is the efficiency of these regular deployment patterns as compared to the optimal pattern? Toward these two questions, we establish the following:

[1]These values of connectivity hold for appropriate internode distances in the four patterns such that each sensor can communicate directly with all its closest neighbors.

- When $\sqrt{2} \leq r_c/r_s \leq \sqrt{3}$, the rhombus-based pattern is better than the other three. It requires upto 21% more sensors as compared to the optimal in this range of r_c/r_s.
- When $1.14 \leq r_c/r_s \leq \sqrt{2}$, the square pattern is better than the other three. It requires upto 60% more sensors than the optimal in this range of r_c/r_s.
- When $r_c/r_s \leq 1.14$, the hexagon pattern is better than the other three. It requires a constant number of sensors for $1 \leq r_c/r_s \leq 1.14$; it uses upto 44% more sensors than the optimal in this range of r_c/r_s.
- When $r_c/r_s < 1$, the number of sensors needed by the hexagon pattern grows exponentially as compared with the optimal. Evidently, the number of sensors needed by the other three patterns are only worse when $r_c/r_s < 1$.

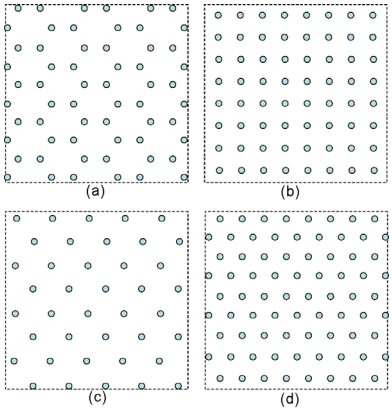

Figure 3: Four common regular patterns of deployment — (a) Hexagon, (b) Square, (c) Rhombus, and (d) Triangular Lattice (with equilateral triangles).

1.2 Applications of Our Results

Aside from the pure theoretical interest, solving the problem of optimal deployment pattern to achieve both coverage and connectivity is important for several reasons.

First, since the sensor nodes still cost close to $100 a piece, deploying the minimum necessary to achieve coverage and connectivity is important for economic reasons. Second, as summarized in Section 1.1, it is now possible to compute, rather precisely, the efficiency of some regular patterns of deployment that may sometimes be used in practice for convenience of deployment. Third, when heuristic algorithms are developed for topology control (i.e., determining a sleep-wakeup schedule for nodes that preserves coverage and/or connectivity) as in [5, 9], it is possible to compute a precise bound on their performance, as compared to the optimal. Fourth, when developing heuristic algorithms for topology control, the insights from the optimal deployment pattern proposed in this paper can be used to improve their performance. For example, the topology control heuristic developed in [9] leveraged the fact that triangular lattice is the optimal deployment pattern when $r_c/r_s \geq 2$. With the new results on optimal deployment pattern to achieve coverage and connectivity developed in this paper, such algorithms may suitably be modified to provide good performance for all ranges of r_c/r_s.

Our results may have other practical utilities. For example, our results may be used to determine the locations of Access Points (AP) when deploying a wireless mesh network. Let the communication range between the AP and clients be considered r_s and that between the APs (assuming they communicate over a different wireless channel) r_c. With this parameter translation, all the applications discussed in the previous paragraph for wireless sensor networks will hold for wireless mesh networks, as well.

1.3 Remarks on the Disk Model

In this paper, we assume that both the sensing and communication ranges are regular disks. In practice, however, it has been discovered that both the sensing and the communication ranges are non-isotropic, i.e., sensors exhibit different ranges (in both sensing and communication) in different directions [11, 10]. According to [3], the passive infrared (PIR) sensor's sensing range in different directions roughly conforms to a Normal Distribution probability model. For the communication range, two non-isotropic models — the Degree of Irregularity (DOI) model and the Radio Irregularity (RIM) model — are presented in [11].

Even though we use a seemingly oversimplified disk model, we believe our results are still applicable in several practical scenarios. For instance, when the irregular sensing and communication ranges each have a lower bound, the sensing and communication areas can be regarded as a disk with radius equal to the lower bound. With this approach, our results can provide a conservative bound on the number of sensors needed to achieve coverage and connectivity deterministically.

We feel that our results probably can be extended to provide statistical coverage guarantees while deterministically ensuring connectivity. To do so, we will need to adopt a statistical sensing range model such as the one proposed in [3], but still using the lower bound on the communication range. We can extend our work further to provide statistical guarantees on both coverage and connectivity based on statistical models such as the ones proposed in [3] and [11]. Extending our results along these lines is part of our future work.

1.4 Related Work

There are three previous works closely related to ours. The asymptotic optimality of triangular lattice was originally proved in [6]. The issue of connectivity, however, was not addressed for $r_c/r_s < \sqrt{3}$.

The strip-based deployment, which we prove to be the optimal for achieving both coverage and 1-connectivity was proposed in both [5] and [7]. In [5], the focus is on the case when $r_c/r_s = 1$. A necessary condition is developed (Theorem 1 in [5]) and it is used to assess the efficiency of the strip-based deployment and of other deployment patterns such as square, hexagon, and triangular lattice. Although the necessary condition developed in this work is close to the optimal when $r_c/r_s \leq 1$ (within 2.7% of the optimal when $r_c/r_s = 1$), it is loose by as much as 30.18%[2].

[2]When $r_c/r_s = \sqrt{3}$, the condition in Theorem 1 of [5] becomes

$$d_{OPT} \geq \frac{1}{r_s^2\left(\frac{2\pi}{3} + \frac{\sqrt{3}}{2}\right)} = \frac{0.5513}{r_s^2},$$

where d_{OPT} is the density of sensors necessary to achieve coverage and connectivity. The density of sensors in the optimal triangular lattice pattern, on the other hand, is $\frac{2}{r_s^2 3\sqrt{3}} = \frac{0.3849}{r_s^2}$.

In [7], the strip-based deployment is carefully constructed for $r_c/r_s < \sqrt{3}$, and it is suggested as the pattern of deployment for this range of r_c/r_s. Neither of these two works ([5, 7]) claim or prove the optimality of the strip-based deployment pattern.

We are not aware of any other work that claim or prove the optimality of the strip-based deployment to achieve coverage and 1-connectivity. Further, we are not aware of any work that consider the problem of determining an optimal deployment pattern to achieve both coverage and 2-connectivity.

Organization of the Paper. The rest of the paper is organized as follows. We list the common assumptions, definitions, and notations that we use throughout the paper in Section 2. In Section 3, we propose the strip-based deployment pattern that achieves coverage and 2-connectivity and prove its asymptotic optimality. In Section 4, we do the same for coverage and 1-connectivity. In Section 5, we establish which regular deployment pattern (out of hexagon, square, rhombus, and equilateral triangle) is better than the others for different ranges of r_c/r_s. In Section 6, we consider an example deployment region and compute the number of nodes needed to achieve coverage and connectivity when different patterns are used. Section 7 concludes the paper.

2. ASSUMPTIONS AND DEFINITIONS

In this section, we describe our model, some assumptions, and key definitions that we use throughout this paper.

ASSUMPTION 2.1. **[Disc-based sensing]** *We assume a disc-based sensing model where each active sensor has a sensing radius of r_s; any object within the disc of radius r_s centered at an active sensor is reliably detected by it. The sensing disk of a sensor located at location u is denoted by $D_{r_s}(u)$.*

ASSUMPTION 2.2. **[Disk-based communication]** *We assume a disc-based radio model where each active sensor has a communication range of r_c; two active sensors at a distance of r_c or less can communicate reliably. The communication disk of a sensor located at location u is denoted by $D_{r_c}(u)$.*

ASSUMPTION 2.3. **[Homogeneous sensing and communication range]** *We assume that the sensing range of all sensors are the same, as are their communication range.*

ASSUMPTION 2.4. **[Bounded value of r_s/r_c]** *We also assume that $\lim_{r_s \to 0} r_s/r_c < M$, for some $M > 0$. The limit $r_s \to 0$ signifies that we need an increasing number of sensors to cover a given region, which is needed for the asymptotic analysis.*

DEFINITION 2.1. **[$d(u,v)$]** *Let the Euclidean distance between points u and v be denoted by $d(u,v)$.*

DEFINITION 2.2. **[Distance between sensing disks]** *For convenience, we define the distance between two sensing disks $D_{r_s}(u)$ and $D_{r_s}(v)$ to be the distance between their centers, $d(u,v)$.*

DEFINITION 2.3. **[Voronoi Polygon, Area Per Node (APN)]** *Let $\{a_1, a_2, ..., a_p\}$ be a set of p points on an Euclidean plane S.*

The **Voronoi polygon** $V(a_i)$ *is the set of all points in* S*, which are closer to* a_i *(in terms of Euclidean distance) than to any other point, i.e.*

$$V(a_i) := \{x \in S : \forall j \in [1, p], d(x, a_i) \leq d(x, a_j)\}.$$

We use **Area Per Node (APN)** *to denote the Lebesgue measure (or area) of a Voronoi polygon.*

DEFINITION 2.4. **[Connected Neighboring Sensors]** *Two sensors located at points* u *and* v *are called* ***connected neighboring sensors****, if*
i) $D_{r_s}(u) \cap D_{r_s}(v) \neq \phi$*, i.e. their sensing disks intersect, and*
ii) $d(u, v) \leq r_c$*.*

Figure 4 illustrates an example for connected neighboring sensors.

DEFINITION 2.5. **[**$\ell(r_s, r_c), \varphi(r_s, r_c)$**]** *Let two connected neighboring sensors be located at* u *and* v*. Then, their sensing disks (*$D_{r_s}(u)$ *and* $D_{r_s}(v)$*) have a common chord (e.g. line segment* AB *in Figure 4). As the locations (*u *and* v*) of the two sensors are varied, the length of their common chord varies as well. A common chord with the smallest possible length (for given values of* r_s *and* r_c*) is called a* ***connection chord,*** *and we denote this minimum length by* $\ell(r_s, r_c)$*. The angles that this common chord of smallest length makes at the centers of* $D_{r_s}(u)$ *and* $D_{r_s}(v)$ *are called* ***connection angles****. We denote these angles by* $\varphi(r_s, r_c)$*.*

Notice that $\ell(r_s, r_c) = 0$ when $r_c \geq 2r_s$.

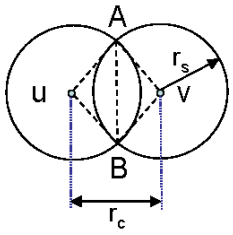

Figure 4: The sensors located at points u **and** v **are connected neighboring sensors with further property that** $d(u, v) = r_c$**. Chord** AB **is the connection chord. And** $\angle AuB$ **and** $\angle AvB$ **are the connection angles.**

DEFINITION 2.6. **[Chord Polygon]** *Consider a deployment of sensors that provides full-coverage. Then, we may assume the sides of the Voronoi polygon generated by every node (except for ones at the boundary) are common chords, since the common area covered by three different sensing disks is expected to be as small as possible in an optimal deployment to achieve one coverage. To emphasize this relationship, we refer to such Voronoi polygons as* ***chord polygons****.*

Note that each chord polygon can be inscribed in a sensing desk D_{r_s}.

DEFINITION 2.7. **[**$A_{k,2}(r_s, r_c)$**]** *Consider a deployment of sensors that provides full-coverage, where every sensor has at least two connected neighboring sensors. Then, for given values of* k*,* r_s*, and* r_c*, the maximum area achievable for a* k*-sided chord polygon (over all possible deployments that provide full-coverage), is denoted by* $A_{k,2}(r_s, r_c)$*.*

The following two definitions are made under the same assumption as in Definition 2.7.

DEFINITION 2.8. **[**$\Phi_{k,n}(r_s, r_c)$**]** *A* k*-sided chord polygon that has* n $(n \leq k)$ *edges of length at least* $\ell(r_s, r_c)$ *is denoted as* $\Phi_{k,n}(r_s, r_c)$*. Its area is denoted as* $|\Phi_{k,n}(r_s, r_c)|$*.*

The following definition refers to a special case of $\Phi_{k,n}(r_s, r_c)$.

DEFINITION 2.9. **[**$\Psi_{k,n}(r_s, r_c)$**]** *A* $\Phi_{k,n}(r_s, r_c)$ *with* n $(n \leq k)$ *edges of length* $\ell(r_s, r_c)$ *and the other* $k - n$ *edges of equal length (not equal to* $\ell(r_s, r_c)$*) is denoted by* $\Psi_{k,n}(r_s, r_c)$*. Its area is denoted by* $|\Psi_{k,n}(r_s, r_c)|$*.*

For brevity, we often use ℓ, φ, $A_{k,2}$, $\Phi_{k,n}$, and $\Psi_{k,n}$ in place of $\ell(r_s, r_c)$, $\varphi(r_s, r_c)$, $A_{k,2}(r_s, r_c)$, $\Phi_{k,n}(r_s, r_c)$, and $\Psi_{k,n}(r_s, r_c)$.

3. OPTIMAL DEPLOYMENT TO ACHIEVE COVERAGE AND 2-CONNECTIVITY

In this section, we present and prove the asymptotic optimality of a strip-based deployment pattern that achieves both full coverage of a square region and forms a 2-connected network. Under this deployment, every point in the square region is covered by at least one sensing disk, and there exist at least 2 node-disjoint (potentially multi-hop) paths between every pair of sensors.

3.1 Strip-based Deployment

The proposed strip-based deployment (see Figure 1) achieves both full coverage of a square region and provides 2-connectivity. It is a variant of the strip-based deployment pattern proposed in [5] and [7] to achieve coverage and 1-connectivity, as illustrated in Figure 2.

Consider a square region of deployment. A horizontal strip of sensors is formed by putting together sensors at a regular separation of $\alpha = \min\{r_c, \sqrt{3}r_s\}$. These strips of sensors are deployed horizontally with alternate rows shifted to the right by a distance of $\alpha/2$. The vertical separation between the neighboring strips is $\beta = r_s + \sqrt{r_s^2 - \alpha^2/4}$. Notice that if $r_c/r_s < \sqrt{3}$, the neighboring horizontal strips are not connected. In this case, we place additional sensors at the left and right boundary of the deployment region (the dark-filled dots in Figure 1). Denote the distance between the sensors at the left boundary of two neighboring horizontal strips by δ, which is equal to $\sqrt{(\alpha/2)^2 + \beta^2}$. Then, we need $2\left(\lceil \delta/r_c \rceil - 1\right)$ sensors to connect a pair of neighboring horizontal strips at both of its boundaries.

3.2 Proof of Optimality

In this section, we prove that the strip-based deployment shown in Figure 1 is asymptotically optimal to achieve coverage and 2-connectivity. The proof borrows several techniques from [6]. For the convenience of readers, we state some key results of [6] in Appendix B.

Let $A_{k,2}(r_s, r_c)$ (or $A_{k,2}$, in short) be as defined in Definition 2.7 and $\varphi(r_s, r_c)$ (or φ, in short) be as defined in Definition 2.5 for given values of r_s and r_c. We first prove some key results that will be used in the proof of optimality.

LEMMA 3.1. *For* $k \geq 3$*,*

$$A_{k,2} = \begin{cases} \frac{r_s^2}{2} k \sin\frac{2\pi}{k}, & \text{when } \frac{2\pi}{k} \geq \varphi \\ r_s^2 \sin\varphi + \frac{r_s^2(k-2)}{2} \sin\frac{2\pi - 2\varphi}{k-2}, & \text{when } \frac{2\pi}{k} < \varphi. \end{cases} \quad (1)$$

PROOF. We only provide a proof sketch here. A rigorous proof can be carried out using the Lagrangian Multiplier Theorem [4].

Consider a deployment as in Definition 2.7. As remarked earlier, each k-sided chord polygon can be inscribed in a sensing disk D_{r_s}. For such a polygon, the maximum area occurs when each of its k sides are of equal length (which is a standard result proved using Lagrangian multipliers). The area of this regular k-sided polygon is $(r_s^2/2)k\sin(2\pi/k)$, and the angle made by each of its edges at its center is $2\pi/k$. When $2\pi/k \geq \varphi$, the regular k-sided polygon satisfies the conditions of Definition 2.7, because $2\pi/k \geq \varphi$ implies that all the k neighboring sensors of D_{r_s} are its connected neighboring sensors. Therefore, $A_{k,2} = (r_s^2/2)k\sin(2\pi/k)$ when $2\pi/k \geq \varphi$.

Now, if $2\pi/k < \varphi$, the angle made by each edge of the regular k-sided polygon at its center is less than φ, and therefore this regular polygon (though having the maximum area of all k-sided polygons inscribed in D_{r_s}) is not formed by any disks that are connected to D_{r_s}, and does not satisfy the conditions of Definition 2.7. In this case, the maximum area of a k-sided chord polygon occurs when the polygon is a $\Psi_{k,2}$. (This claim can again be proved using the Lagrangian multipliers). We refer to such a polygon as a semi-regular one. In this case,

$$A_{k,2} = r_s^2 \sin\varphi + \frac{r_s^2}{2}(k-2)\sin\frac{2\pi-2\varphi}{k-2}.$$

This completes the proof. □

The next lemma, which uses the results of Lemma 3.1, is analogous to Lemma 2 of [6] (see Appendix B).

LEMMA 3.2. *For $k \geq 4$,*

$$0 < A_{k+1,2} - A_{k,2} < A_{k,2} - A_{k-1,2}. \tag{2}$$

PROOF. We divide our proof obligation into four cases.

Case 1: $\varphi \leq 2\pi/(k+1)$. In this case, as proved in Lemma 3.1, $A_{k+1,2}$, $A_{k,2}$ and $A_{k-1,2}$ all involve regular chord polygons. Therefore, (2) follows from Lemma 2 in [6].

Case 2: $\varphi \geq 2\pi/(k-1)$. In this case, as proved in Lemma 3.1,

$$A_{i,2} = r_s^2 \sin\varphi + \frac{r_s^2}{2}(i-2)\sin\frac{2\pi-2\varphi}{i-2}$$

for $i = k-1, k, k+1$. The first inequality in (2) can be easily proved using Taylor's expansion for $\sin x$. We now prove the second inequality. Defining $f(k) = A_{k+1,2} - A_{k,2}$, we have

$$f(k) = \frac{k-1}{2}r_s^2 \sin\frac{2\pi-2\varphi}{k-1} - \frac{k-2}{2}r_s^2\sin\frac{2\pi-2\varphi}{k-2}. \tag{3}$$

Taking derivatives of both sides of (3), we get

$$\begin{aligned}\frac{df(k)}{dk} &= \frac{r_s^2}{2}\left[\sin\frac{2\pi-2\varphi}{k-1} - \frac{2\pi-2\varphi}{k-1}\cos\frac{2\pi-2\varphi}{k-1}\right] \\ &- \frac{r_s^2}{2}\left[\sin\frac{2\pi-2\varphi}{k-2} - \frac{2\pi-2\varphi}{k-2}\cos\frac{2\pi-2\varphi}{k-2}\right].\end{aligned}$$

Since $\sin x - x\cos x$ is an increasing function of x in $(0,\pi)$ and $(2\pi-2\varphi)/(k-1), (2\pi-2\varphi)/(k-2) \in (0,\pi)$ for $k \geq 4$, $df(k)/dk < 0$ for $k \geq 4$. Hence, $f(k)$ is a decreasing function, and thus (2) holds when $2\pi/(k-1) \leq \varphi$.

Case 3: $2\pi/(k+1) < \varphi \leq 2\pi/k$. For $k \geq 3$, let $A_{k,2}^r$ denote the area of a regular k-sided chord polygon, and $A_{k,2}^s$ the area of a semi-regular k-sided chord polygon. That is,

$$A_{k,2}^r = \frac{r_s^2}{2}k\sin\frac{2\pi}{k}$$

and

$$A_{k,2}^s = r_s^2\sin\varphi + \frac{r_s^2(k-2)}{2}\sin\frac{2\pi-2\varphi}{k-2}.$$

In this case (case 3), $A_{k+1,2} = A_{k+1,2}^s$, $A_{k,2} = A_{k,2}^r$, and $A_{k-1,2} = A_{k-1,2}^r$. For the first inequality in (2), we have

$$\begin{aligned}&A_{k+1,2}^s - A_{k,2}^r \\ =\ & \frac{k-1}{2}r_s^2\sin\frac{2\pi-2\varphi}{k-1} + r_s^2\sin\varphi - \frac{k}{2}r_s^2\sin\frac{2\pi}{k}\end{aligned}$$

which is greater than 0 for $2\pi/(k+1) < \varphi \leq 2\pi/k$.

For the second inequality in (2), we need to prove

$$A_{k+1,2}^s - A_{k,2}^r < A_{k,2}^r - A_{k-1,2}^r,$$

which follows from Lemma 2 in [6] and the fact that $A_{k+1,2}^s < A_{k+1,2}^r$ (the latter inequality holds since $A_{k+1,2}^s$ is the maximum area possible of any $(k+1)$-sided polygon inscribed in D_{r_s}).

Case 4: $2\pi/k < \varphi < 2\pi/(k-1)$. In this case, for the first inequality in (2), $0 < A_{k+1,2}^s - A_{k,2}^s$ can be proved using Taylor's expansion for $\sin x$. For the second inequality in (2), we need to prove

$$A_{k+1,2}^s - A_{k,2}^s < A_{k,2}^s - A_{k-1,2}^r,$$

which follows from the fact that

$$\begin{aligned}&(A_{k,2}^s - A_{k-1,2}^r) - (A_{k+1,2}^s - A_{k,2}^s) \\ =\ & (k-2)r_s^2\sin\frac{2\pi-2\varphi}{k-2} - \frac{r_s^2}{2}(k-3)\sin\frac{2\pi}{k-1} \\ & -\frac{r_s^2}{2}(k-1)\sin\frac{2\pi-2\varphi}{k-1}\end{aligned}$$

is greater than 0, for $2\pi/k < \varphi < 2\pi/(k-1)$.

The four cases together prove (2) for all values of φ. □

The next lemma, which uses the results of Lemma 3.2, is analogous to Lemma 4 of [6].

LEMMA 3.3. *Let Γ denote a set of non-overlapping F finite polygons that fully cover a bounded plane. Suppose that each vertex of Γ is on at least three edges. Further, suppose that the area of each k-sided polygon of Γ is at most $A_{k,2}$, where $A_{k,2}$ is as defined in Definition 2.7. Then, the total area of Γ, denoted by A_Γ, satisfies*

$$A_\Gamma < FA_{6,2},$$

where (using (1))

$$A_{6,2} = \begin{cases} \frac{3\sqrt{3}}{2}r_s^2, & \text{when } \frac{\pi}{3} \geq \varphi \\ r_s^2\sin\varphi + 2r_s^2\sin\frac{\pi-2\varphi}{2}, & \text{when } \frac{\pi}{3} < \varphi \end{cases} \tag{4}$$

PROOF. The proof of this Lemma can be carried out in the same manner as in Lemma 4 of [6] using Lemma 3.2 in place of Lemma 2 of [6] and using $A_{6,2}$ in place of A_6 in [6]. □

The next lemma, which uses Lemma 3.3, provides a lower bound on the number of sensors needed to cover a rectangle while forming a 2-connected network.

LEMMA 3.4. *Let ρ denote a rectangle in the plane with area R. Let $N(r_s, r_c)$ denote the minimum number of sensing disks*

D_{r_s} which can cover ρ and the centers of which form a 2-connected network using the communication radius r_c. Then

$$\pi r_s^2 N(r_s, r_c) > \begin{cases} (R - 2\pi r_s^2)(2\pi\sqrt{3}/9), & \text{when } \frac{\pi}{3} \geq \varphi \\ \pi(R - 2\pi r_s^2)(\sin\varphi + 2\sin\frac{\pi - 2\varphi}{2})^{-1}, & \text{when } \frac{\pi}{3} < \varphi \end{cases}$$

PROOF. To prove this lemma, we apply Lemma 3.3 after showing that the two hypotheses made there are satisfied by the set of Voronoi polygons (see Definition 2.3) generated by the centers of the disks and the boundary of ρ. These Voronoi polygons are non-overlapping and cover ρ.

These polygons satisfy the first hypothesis of Lemma 3.3 (namely, each vertex of the Voronoi polygons is on at least three edges) if we follow the same technique as in the proof of Lemma 5 of [6] that chops off the four corners of ρ. This construction reduces the area of ρ by less than $2\pi r_s^2$. Therefore,

$$A_\Gamma \geq R - 2\pi r_s^2, \tag{5}$$

where A_Γ is as defined in the statement of Lemma 3.3.

To see how the second hypothesis of Lemma 3.3 (namely, the area of each k-sided Voronoi polygon is at most $A_{k,2}$) is satisfied, we argue as follows. Since the $N(r_s, r_c)$ disks completely cover the rectangle ρ and the centers of these disks form a 2-connected network, the center of each disk is at a distance of less than r_c of at least two neighboring disks. Therefore, by the definition of $A_{k,2}$, the area of each Voronoi polygon is at most $A_{k,2}$.

Since there is a one-to-one mapping between Voronoi polygons and the disks D_{r_s}, there are $N(r_s, r_c)$ Voronoi polygons covering ρ. Using (5) and applying Lemma 3.3, we obtain

$$R - 2\pi r_s^2 < N(r_s, r_c) A_{6,2}, \tag{6}$$

where $A_{6,2}$ is as defined in (4). Multiplying both sides of (6) by $\pi r^2 / A_{6,2}$ and then applying (4), we get (5). □

We now derive the asymptotically optimal number of sensors needed to provide full-coverage and 2-connectivity.

THEOREM 3.1. *Let $N(r_s, r_c)$ denote the minimum number of sensing disks, D_{r_s}, which can cover a square with area L^2, and the centers of which form a 2-connected network using the communication radius r_c. Then,*

$$\lim_{r_s \to 0} \pi r_s^2 N(r_s, r_c) = K(r_s, r_c) L^2, \tag{7}$$

where

$$K(r_s, r_c) = \begin{cases} 2\pi\sqrt{3}/9, & \text{when } \frac{\pi}{3} \geq \varphi \\ \pi(\sin\varphi + 2\sin\frac{\pi - 2\varphi}{2})^{-1}, & \text{when } \frac{\pi}{3} < \varphi \end{cases}$$

PROOF. To prove (7), we need to prove

$$\liminf_{r_s \to 0} \pi r_s^2 N(r_s, r_c) \geq K(r_s, r_c) L^2, \tag{8}$$

and

$$\limsup_{r_s \to 0} \pi r_s^2 N(r_s, r_c) \leq K(r_s, r_c) L^2. \tag{9}$$

Using Lemma 3.4 in place of Lemma 5 of [6] in the proof of Theorem in [6], we get the proof of (8).

We will now prove (9) using the strip based construction shown in Figure 1.

Let $N'(r_s, r_c)$ be the number of disks needed in the strip based deployment. It can be verified that this deployment provides coverage of the square and the centers of the disks form a 2-connected network. Therefore, we have

$$N(r_s, r_c) \leq N'(r_s, r_c). \tag{10}$$

Multiplying both sides of (10) by πr^2, and taking limit as $r_s \to 0$, we obtain

$$\limsup_{r_s \to 0} \pi r_s^2 N(r_s, r_c) \leq \lim_{r_s \to 0} \pi r_s^2 N'(r_s, r_c)$$

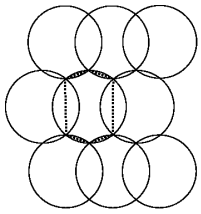

Figure 5: One of the non-overlapping hexagons that tile the plane.

We divide $N'(r_s, r_c)$ into two parts — $N'_h(r_s, r_c)$ that denotes the number of disks in all the horizontal strips (see Figure 1), and $N'_v(r_s, r_c)$ that denotes the number of disks in the two vertical strips, so that

$$N'_h(r_s, r_c) + N'_v(r_s, r_c) = N'(r_s, r_c). \tag{11}$$

Note that $N'_v(r_s, r_c) = 0$ when $\pi/3 \geq \varphi$ (i.e. $r_c \geq \sqrt{3} r_s$).

To derive an expression for $N'_h(r_s, r_c)$, we observe that the entire square is tiled with non-overlapping hexagons such as the one shown with dotted lines in Figure 5. It can be shown that the area of each such hexagon is $A_{6,2}$ (defined in (4)). Therefore, we have

$$\lim_{r_s \to 0} \pi N'_h(r_s, r_c) A_{6,2} = \pi L^2,$$

which can be rewritten (using (1)) as

$$\lim_{r_s \to 0} \pi N'_h(r_s, r_c) r_s^2 = K(r_s, r_c) L^2, \tag{12}$$

where $K(r_s, r_c)$ is as defined in the statement of this theorem.

For $N'_v(r_s, r_c)$,

$$N'_v(r_s, r_c) \pi r_s^2 < 2\left(\frac{L}{r_c} + 1\right) \pi r_s^2 = 2\pi r_s \left(L \frac{r_s}{r_c} + 1\right), \tag{13}$$

which follows from the construction of the strip-based deployment. As $r_s \to 0$, the right hand side of (13) approaches zero, as well, as r_s / r_c is bounded. Hence,

$$\limsup_{r_s \to 0} \pi r_s^2 N'_v(r_s, r_c) = 0. \tag{14}$$

Using (11), (12), and (14), we obtain

$$\lim_{r_s \to 0} \pi r_s^2 N'(r_s, r_c) = K(r_s, r_c) L^2,$$

which together with (10) proves (9). □

The next theorem, which follows immediately from the proof of Theorem 3.1, proves the optimality of the strip-based deployment presented in Figure 1.

THEOREM 3.2. *The strip based deployment, as described in Section 3.1 and shown in Figure 1 is an asymptotically optimal deployment pattern to achieve 2-connected-cover.*

4. OPTIMAL DEPLOYMENT TO ACHIEVE COVERAGE AND 1-CONNECTIVITY

In this section, we prove the asymptotic optimality of the strip-based deployment (shown in Figure 2) that was proposed in both [5] and [7] to achieve coverage and 1-connectivity when $r_c/r_s < \sqrt{3}$. The construction of the strip-based deployment pattern for coverage and 1-connectivity is the same as the strip-based deployment pattern to achieve coverage and 2-connectivity, presented in Section 3.1, except for two differences. First, only one vertical strip is needed here. Second, the vertical strip need not connect the horizontal strip at their boundaries. We note that when $r_c/r_s \geq \sqrt{3}$, the triangular lattice [6] is the optimal deployment pattern to achieve both coverage and connectivity.

We now state a simple result that we use later in the proofs.

LEMMA 4.1. *Let $p_1, p_2, \ldots, p_n$ be points on a plane and for each pair i, j with $1 \leq i, j \leq n$, we say that p_i and p_j are connected if $d(p_i, p_j) \leq C$, where $C > 0$ is a constant. Let m_i be the number of points $p_j \neq p_i$ such that $d(p_i, p_j) \leq C$. If $p_1, p_2, \ldots, p_n$ form a connected network, i.e., there exists at least one path between every pair of points, then for $n \geq 2$,*

$$\sum_{i=1}^{n} \frac{m_i}{n-1} \geq 2 \tag{15}$$

By Lemma 4.1, as $n \to \infty$, the average number of m_i is at least 2. Therefore, it is not surprising that we get very similar optimal deployment patterns for providing coverage and 1-connectivity as for providing coverage and 2-connectivity.

However, since having two connected neighboring sensors is not necessary to achieve 1-connectivity, the method for proving the necessity of the deployment (shown in Figure 2) for achieving coverage and 1-connectivity is more involved.

Let $\varphi, \Phi_{k,n}, \Psi_{k,n}$ be as defined in Section 2. The following lemma is a key result towards proving the asymptotic optimality for coverage and 1-connectivity.

LEMMA 4.2. *Consider a deployment of m sensors that provides both coverage and 1-connectivity. Let $\{\Phi_{k_i,n_i} : 1 \leq i \leq m\}$ be the set of k-sided chord polygons generated by this deployment. If this set satisfies the following conditions for $r_c/r_s < \sqrt{3}$ (i.e., $\pi/3 < \varphi < \pi$):*
(1) $\sum_{i=1}^{m} k_i \leq 6m$,
(2) $\sum_{i=1}^{m} n_i \geq 2m$,
(3) $\forall 1 \leq i \leq m$, $n_i \geq 1$
then $\sum_{i=1}^{m} |\Phi_{k_i,n_i}|$ attains its maximum (over all deployments that achieve coverage and 1-connectivity) when Φ_{k_i,n_i} ($\forall 1 \leq i \leq m$) is an $\Psi_{6,2}$.

See Appendix A for a proof of Lemma 4.2. The following theorem states the number of sensors necessary for providing coverage with 1-connectivity.

THEOREM 4.1. *Let $N(r_s, r_c)$ be the minimum number of sensing disks, D_{r_s}, which cover a square with area L^2 and the centers of which (sensors) form a 1-connected network using r_c. If $r_c/r_s < \sqrt{3}$, then*

$$\lim_{r_s \to 0} \pi r_s^2 N(r_s, r_c) = \pi \left(\sin\varphi + 2\sin\frac{\pi - 2\varphi}{2} \right)^{-1} L^2. \tag{16}$$

PROOF. To prove (16), we need to prove

$$\liminf_{r_s \to 0} \pi r_s^2 N(r_s, r_c) \geq \pi \left(\sin\varphi + 2\sin\frac{\pi - 2\varphi}{2} \right)^{-1} L^2 \tag{17}$$

and

$$\limsup_{r_s \to 0} \pi r_s^2 N(r_s, r_c) \leq \pi \left(\sin\varphi + 2\sin\frac{\pi - 2\varphi}{2} \right)^{-1} L^2. \tag{18}$$

We use Lemma 4.2 to prove (17). Consider a deployment that uses $N(r_s, r_c)$ sensors to provide full coverage and connectivity. Let $\{\Phi_{k_i,n_i} : 1 \leq i \leq N(r_s, r_c)\}$ be the set of k-sided chord polygons generated by this deployment. Since this deployment provides full coverage, we have

$$\sum_{i=1}^{N(r_s,r_c)} |\Phi_{k_i,n_i}| \geq L^2. \tag{19}$$

Observe that the three conditions stated in Lemma 4.2 are satisfied by this deployment. Lemma 1 in [6] ensures that condition (1) is satisfied by all deployments that provide full coverage. Lemma 4.1 ensures that condition (2) is satisfied by all deployments that provide 1-connectivity. Condition (3) is trivially satisfied by all deployments that provide connectivity. Applying Lemma 2, we obtain

$$\sum_{i=1}^{N(r_s,r_c)} |\Psi_{6,2}| \geq \sum_{i=1}^{N(r_s,r_c)} |\Phi_{k_i,n_i}|. \tag{20}$$

Using (19), (20), and the fact that $|\Psi_{6,2}| = r_s^2(\sin\varphi + 2\sin\frac{\pi-2\varphi}{2})$, we obtain (21), which yields (17).

$$N(r_s, r_c) r_s^2 \left(\sin\varphi + 2\sin\frac{\pi - 2\varphi}{2} \right) \geq L^2, \tag{21}$$

The proof of (18) closely follows the proof of (9) in the proof of Theorem 3.1. When $r_c/r_s < \sqrt{3}$ so that $\pi/3 < \varphi$, $|\Psi_{6,2}| = A_{6,2}$. Therefore, when $r_c/r_s < \sqrt{3}$, (18) reduces to (9). Further, since the strip-based deployment presented in Figure 2 asymptotically needs the same number of sensors as that of Figure 1, (18) follows from the proof of (9). □

The next theorem, which follows immediately from the proof of Theorem 4.1, proves the optimality of the strip-based deployment presented in Figure 2.

THEOREM 4.2. *The strip based deployment, shown in Figure 2, is asymptotically optimal for achieving coverage and connectivity, when $r_c/r_s < \sqrt{3}$.*

5. HOW GOOD ARE SOME REGULAR DEPLOYMENT PATTERNS?

In this section, we consider four popular regular patterns of deployment — hexagon, square grid, rhombus, and equilateral triangle (all of which are shown in Figure 3). These patterns are often used in practice for convenience of deployment (or to achieve a higher degrees of connectivity). We address the following two questions in this regard — (1) which of these regular patterns is more efficient than the others (in terms of the number of sensors needed)? (2) what is the efficiency of these regular deployment patterns as compared to the optimal pattern? We comprehensively address the first of these questions in Section 5.1 and the second in Section 6.

5.1 Efficiency of Some Regular Deployment Patterns

In a regular topology (composed of homogeneous patterns), the area of the *APN* (see Definition 2.3), denoted by γ, can be

computed as follows:

$$\gamma = \frac{A_p}{N_p} \cdot N_n, \tag{22}$$

where A_p is the area of the pattern, N_p denotes the number of nodes that compose a pattern, and N_n denotes the number of pattern blocks that share a node. For example, as shown in Figure 6, in a hexagon pattern, $N_p = 6$ and $N_n = 3$; in a triangular lattice pattern, $N_p = 3$ and $N_n = 6$; and in a square pattern, $N_p = 4$ and $N_n = 4$.

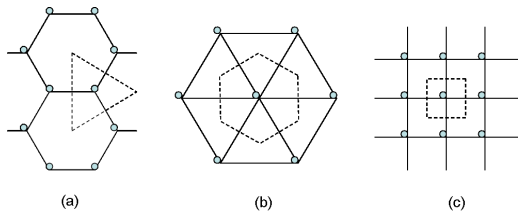

Figure 6: Regular pattern based networks, (a) A hexagon pattern is composed of 6 nodes, and any single node is shared by 3 pattern blocks. (b) An equilateral pattern is composed of 3 nodes and any single nodes is shared by 6 pattern blocks. (c) A square pattern is composed of 4 nodes, and any single node is shared by 4 pattern blocks. The polygons with the dotted line are Voronoi Polygons in different deploy pattern.

We now state a lemma for ease of reference. A simple, convex polygon whose vertices all lie on its circumcircle is said to be a *cyclic polygon*. (For instance, all regular simple polygons, all triangles, and all rectangles are cyclic.)

LEMMA 5.1. *Let sensors be deployed at the vertices of a cyclic polygon P. If P's circumcenter falls in its interior, then the polygonal region (enclosed by P) is fully covered by the sensors iff P's circumcenter is covered.*

PROOF. The "only if" part is obvious. For the "if" part, let P be any cyclic polygon with its circumcenter, o, inside the polygon. Assume o is covered. Then the sensing range satisfies $r_s \geq d(o, v)$ for any vertex v in P. Let $x \neq o$ be any point inside the polygon. There is an edge (a, b) on P such that x is inside (or on the boundary of) the triangle abo. Evidently, either $d(x, a) \leq d(o, a)$ or $d(x, b) \leq d(o, b)$. Thus, x is covered by at least one of the sensors at a and b. This proves the lemma. □

Since *APN* denotes the average contribution of each node to the coverage in a regular pattern based topology, we use it to determine the efficiency of a pattern. For each pattern, we want to maximize its *APN*, while guaranteeing that each point in the deployment region is covered and the network is connected. According to Lemma 5.1, it can be shown that the maximum *APNs* for the regular hexagon-based topology, square grid topology, and the triangular lattice topology, denoted by $\gamma^H_{max}, \gamma^S_{max}, \gamma^T_{max}$ respectively, are given by the following expressions:

$$\gamma^H_{max} = \frac{3}{4}\sqrt{3}(\min\{r_c, r_s\})^2 \tag{23}$$

$$\gamma^S_{max} = 2\left(\min\left\{r_s, \frac{\sqrt{2}}{2}r_c\right\}\right)^2 \tag{24}$$

$$\gamma^T_{max} = \frac{3}{2}\sqrt{3}\left(\min\left\{r_s, \frac{\sqrt{3}}{3}r_c\right\}\right)^2 \tag{25}$$

We now derive the maximum *APN* for the rhombus-based topology, denoted by γ^R_{max}. Observe that a rhombus can be divided into two congruent acute isosceles triangles as shown in Figure 7[3]. Also, observe that when the acute angle of a rhombus is $\pi/2$, we get a square. Therefore, the grid topology, which is based on a square pattern, is a special case of the rhombus-based topology. Similarly, when we set the acute angle of a rhombus equal to $\pi/3$, we get two equilateral triangles composing the rhombus. In this case, the rhombus-based topology becomes a triangular lattice topology (which is composed of equilateral triangles).

THEOREM 5.1. *Let $\gamma^R(r_c, r_s, \theta)$ denote the* APN *in a rhombus-based topology with acute angle θ that provides both coverage and connectivity with a communication radius of r_c and a sensing radius of r_s. Then,*

$$\gamma^R(r_c, r_s, \theta) = \alpha^2(r_c, r_s, \theta)\sin\theta \tag{26}$$

where $\alpha(r_s, r_c, \theta) = \min\{r_c, 2r_s\cos\frac{\theta}{2}\}$. The maximum value of $\gamma^R(r_c, r_s, \theta)$, γ^R_{max}, occurs at $\theta = \frac{\pi}{2}$ when $\frac{r_c}{r_s} \leq \sqrt{2}$, at $\theta = \pi - 2\arcsin\frac{r_c}{2r_s}$ when $\sqrt{2} \leq \frac{r_c}{r_s} \leq \sqrt{3}$, and at $\theta = \frac{\pi}{3}$, when $\sqrt{3} \leq \frac{r_c}{r_s}$.

PROOF. To maximize the *APN* of a rhombus-based pattern, it is sufficient to maximize the area of the rhombus. This is because for $\theta > \pi/3$, $N_n/N_p = 1$, and therefore *APN* is the same as A_p, the area of the rhombus pattern. For $\theta \leq \pi/3$, the rhombus pattern deployment can be considered a deployment in the triangular pattern since the three sensors making up a triangle are within a distance of r_c or less of each other. In this case, $N_n/N_p = 2$, and therefore *APN* is the same as twice the area of a triangle, which is same as the area of a rhombus.

Now, any rhombus can be divided into two congruent acute isosceles triangles. Therefore, to maximize the area of a rhombus, it is sufficient to maximize the area of each of its isosceles triangles. Without loss of generality, we consider one of these isosceles triangles, as shown in Figure 7. In Figure 7, we consider the triangle abc so that $\angle abc = \theta$.

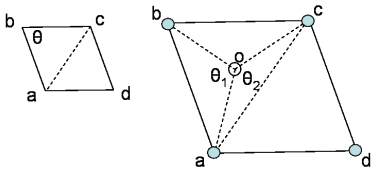

Figure 7: half of the rhombus pattern with d, θ_1 and θ_2

The point o in Figure 7 is the circumcenter of the triangle abc. Let d be the length of the radius of the circumcircle for the triangle abc. This implies that $d(o, a) = d(o, b) = d(o, c) = d$.

[3]We consider an isosceles triangle an acute isosceles triangle if every angle of this triangle is at most $\pi/2$.

By Lemma 5.1, we know that in order for the sensors located at the vertices of the triangle abc, the circumcenter o must be covered by each. Therefore, to achieve full-coverage, we must have

$$d \leq r_s \tag{27}$$

To achieve connectivity, we must have $d(a,b) \leq r_c$. This constraint holds even if $d(a,c) < d(a,b)$; otherwise connectivity in the horizontal direction will not be ensured. Let $\angle aob = \theta_1$, then $\theta_1 = \pi - \theta$. The constraint $d(a,b) \leq r_c$ can be now rewritten as

$$d \leq \frac{r_c}{2y}, \tag{28}$$

where $y = \sin(\theta_1/2)$.

Now, we find the maximum value of the area of the triangle abc while satisfying the constraints (27) and (5.1). Let $\angle aoc = \theta_2$. Then, the area of this triangle, A_t, is given by

$$A_t = \frac{1}{2}d^2(\sin(\theta_1) + \sin(\theta_1) + \sin(\theta_2)). \tag{29}$$

Using the fact that θ_1 and θ_2 satisfy: $2\theta_1 + \theta_2 = \pi$ and with some calculation, (29) can be rewritten as

$$A_t = 4d^2y^3\sqrt{1-y^2}, \tag{30}$$

where $0 < y = \sin(\theta_1/2) < 1$.

We consider two cases for maximizing A_t while satisfying the constraints (27) and (5.1) —

[Case 1]: When $r_s \leq r_c/2y$, only constraint (27) need be considered i.e. $d \leq r_s$. The objective function A_t can now be considered as the product of two independent functions $A_t = f(d)g(y)$, where $f(d) = 4d^2$ and $g(y) = y^3\sqrt{1-y^2}$.

Since both $f(d)$ and $g(y)$ are positive functions, we can maximize them separately to maximize the objective function A_t. The function $f(d)$ is maximized when $d = r_s$, because $f(d)$ is a monotonically increasing function on $0 < d \leq r_s$. The function $g(y)$ is a concave for $0 < y < 1$, achieving its maximum when $y = \sqrt{3}/2$. So, $g(y)$ is increasing when $0 < y \leq \sqrt{3}/2$ and decreasing when $\sqrt{3}/2 \leq y < 1$. There are two constraints on $y : 0 < y < 1$ and $y \leq r_c/2r_s$. Therefore, $g(y)$ attains its maximum at $y = \min(r_c/2r_s, \sqrt{3}/2)$.

Hence, we obtain if $r_c/2r_s \leq \sqrt{3}/2$, A_t is maximized when $y = r_c/2r_s$, and if $r_c/2r_s \geq \sqrt{3}/2$, A_t is maximized when $y = \sqrt{3}/2$.

[Case 2:] When $r_s \geq r_c/2y$, only (5.1) needs to be considered, i.e. $d \leq r_c/2y$. Then the maximum value of A_t occurs at a value of y that maximizes $h(y) = r_c^2 y\sqrt{1-y^2}$.

The function $h(y)$ is concave when $0 < y < 1$ attaining its maximum when $y = \sqrt{2}/2$. Further, $h(y)$ increases in the interval $0 < y < \sqrt{2}/2$, and decreases in the interval $\sqrt{2}/2 < y < 1$. From the constraint, $r_s \geq r_c/2y$, we get that $y \geq r_c/2r_s$. Therefore, A_t attains its maximum when $y = \max(r_c/2r_s, \sqrt{2}/2)$.

Hence, in this case, we obtain that if $r_c/2r_s \leq \sqrt{2}/2$, A_t is maximized when $y = \sqrt{2}/2$, and if $r_c/2r_s \geq \sqrt{2}/2$, A_t is maximized when $y = r_c/2r_s$.

By combining the two cases, we obtain that if $r_c/r_s \leq \sqrt{2}$, γ^R_{max} occurs when $y = \sqrt{2}/2$, if $\sqrt{2} \leq r_c/r_s \leq \sqrt{3}$, γ^R_{max} occurs when $y = r_c/2r_s$, and if $r_c/r_s \geq \sqrt{3}$, γ^R_{max} occurs when $y = \sqrt{3}/2$. The theorem now follows by noting that $y = \sin\theta_1/2$, which can be rewritten as $\theta_1 = 2\arcsin(y)$, and recalling that $\theta_1 = \pi - \theta$. The later relation can be rewritten in terms of y as $\theta = \pi - 2\arcsin(y)$. □

Now we state a theorem that summarizes which regular pattern is better than the other three for different ranges of r_c/r_s.

THEOREM 5.2. *Consider a network of homogeneous sensors with sensing radius r_s and communication radius r_c deployed over a unit square region that is required to provide both full-coverage and connectivity. Let γ_{max} be the maximum APN of the four regular deployment patterns — hexagon, square, rhombus, and triangular lattice. Then,*

$$\gamma_{max} = \begin{cases} \gamma^H_{max}, & \text{when } 0 < \frac{r_c}{r_s} \leq \frac{1}{2}3^{\frac{3}{4}}, \\ \gamma^S_{max}, & \text{when } \frac{1}{2}3^{\frac{3}{4}} \leq \frac{r_c}{r_s} \leq \sqrt{2}, \\ \gamma^R_{max}, & \text{when } \sqrt{2} \leq \frac{r_c}{r_s} \leq \sqrt{3}, \\ \gamma^T_{max}, & \text{when } \sqrt{3} \leq \frac{r_c}{r_s}, \end{cases} \tag{31}$$

where $\gamma^H_{max}, \gamma^S_{max}, \gamma^R_{max}$, and γ^T_{max} are defined in (23)*,* (24)*,* (26)*, and* (25)*, respectively.*

PROOF. We prove the theorem by comparing the values of $\gamma^H_{max}, \gamma^S_{max}, \gamma^R_{max}$, and γ^T_{max} for different values of r_c/r_s.

We rewrite the *APNs* as follows:

$$\gamma^H_{max} = \frac{3}{4}\sqrt{3}r_s^2\left(\min\left\{1, \frac{r_c}{r_s}\right\}\right)^2 \tag{32}$$

$$\gamma^S_{max} = r_s^2\left(\min\left\{\sqrt{2}, \frac{r_c}{r_s}\right\}\right)^2 \tag{33}$$

$$\gamma^T_{max} = \frac{\sqrt{3}}{2}r_s^2\left(\min\left\{\sqrt{3}, \frac{r_c}{r_s}\right\}\right)^2 \tag{34}$$

When $r_c/r_s \leq \sqrt{2}$ the rhombus pattern reduces to a square and so that $\gamma^R_{max} = \gamma^S_{max}$. When $\sqrt{3} \leq r_c/r_s$, the rhombus pattern reduces to the triangular lattice so that $\gamma^R_{max} = \gamma^T_{max}$. So, we only need to determine γ^R_{max} when $\sqrt{2} \leq r_c/r_s \leq \sqrt{3}$. In this case γ^R_{max} occurs at $\theta = (\pi - 2\arcsin(r_c/2r_s))$ so that $2\cos(\theta/2) = r_c/r_s$. Now, γ^R_{max} can be rewritten as

$$\gamma^R_{max} = r_c^2\sin(\theta), \tag{35}$$

where $\pi/3 \leq \theta \leq \pi/2$ and $\sqrt{2} \leq r_c/r_s \leq \sqrt{3}$.

Now, if $r_c/r_s \leq 1$, clearly, γ^R_{max} does not apply and γ^H_{max} is greater than the other two. Also, notice that from the condition of Theorem 5.1, rhombus reduces to a square, if $r_c/r_s \leq \sqrt{2}$. Therefore, in this case, the hexagonal deployment is the best deployment pattern. We will now explore for what further values of r_c/r_s hexagonal pattern continues to beat other patterns. When $r_c/r_s \in [1, \sqrt{2}]$, notice that $\gamma^S_{max} > \gamma^T_{max}$. So, we only need to compare γ^H_{max} with γ^S_{max}. Notice that when $r_c/r_s \in [1, \sqrt{2}]$, $\gamma^H_{max} = 3\sqrt{3}r_s^2/4$ and $\gamma^S_{max} = r_s^2(r_c/r_s)^2$, which implies that $\gamma^H_{max} \geq \gamma^S_{max}$, when $r_c/r_s \leq \sqrt{3\sqrt{3}/4} = \frac{1}{2}3^{\frac{3}{4}}$.

Similar calculation yields the other three conditions. □

6. NUMERICAL COMPUTATION

In this section, we compare the number of nodes needed to provide both coverage and connectivity over a deployment region of size $1,000m \times 1,000m$ with $r_s = 30m$, and $24m \leq r_c \leq 75m$, when different patterns are used[4]. To determine the number of nodes needed in each of the four regular patterns of deployment (hexagon, square, rhombus, and equilateral triangle), we divide the area of the deployment region by

[4]For simplicity, we do not consider the number of nodes needed to cover the boundary of the deployment region.

the maximum *APN* (see Definition 2.3 and (22)) of the corresponding patterns. For the optimal strip-based deployment patterns, we use the construction provided in Section 3.1 and in the first paragraph of Section 4 to compute the number of nodes needed by them. Figure 8 shows the results of our computation.

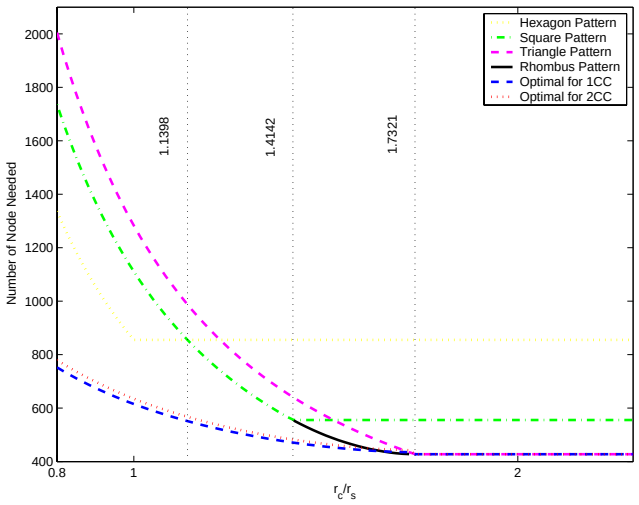

Figure 8: Number of nodes needed in the different patterns of deployment (hexagon, square, rhombus, triangle, and the optimal strip-based deployment patterns)to achieve both coverage and connectivity for various values of r_c/r_s, when sensors each with $r_s = 30m$ are deployed over a $1,000m \times 1,000m$ deployment region. The communication range r_c is varied from 24 m to 75 m.

We make the following observations. First, the number of nodes needed by the two strip based deployments (shown in Figure 1 and Figure 2) are close. In our example, and for $r_c/r_s = 0.8$, they differ by approximately 3%. In general, the optimal deployment pattern to achieve coverage and 2-connectivity requires κ additional nodes in a square deployment region of length L, as compared to the optimal deployment pattern for coverage and 1-connectivity, where $\kappa = (L/\beta)\left(\lceil \delta/r_c \rceil - 1\right)$, using the definitions from Section 3.1. Second, regular deployment patterns, while using some extra nodes over the optimal, can provide a higher degree of connectivity than the optimal strip-based patterns when $r_c/r_s < \sqrt{3}$. Finally, out of the four regular patterns of deployment we consider, no pattern is the best for all values of r_c/r_s. More concretely, the following holds:

1. When $r_c/r_s \geq \sqrt{3}$, the triangle based pattern is optimal to achieve both coverage and connectivity. In fact, it provides 6-connectivity for this range of r_c/r_s.

2. When $\sqrt{2} \leq r_c/r_s \leq \sqrt{3}$, the rhombus-based pattern provides coverage and 4-connectivity, while requiring at most 21% more nodes than the optimal. This implies that for this range of r_c/r_s, coverage and 4-connectivity can be achieved by deploying less than 21% extra nodes, provided they are deployed in a rhombus-based pattern.

3. When $1.1398 \leq r_c/r_s \leq \sqrt{2}$, the square grid pattern provides coverage and 4-connectivity, but the number of sensors it needs over the optimal start to increase sharply with a decrease in the value of r_c/r_s. It suggests that using the square grid pattern may be expensive (requiring upto 60% more than the optimal) when $r_c/r_s < 1.14$.

4. For $r_c/r_s < 1.14$, hexagon pattern provides coverage and 3-connectivity. The number of nodes needed by the hexagon pattern remains constant for $1 \leq r_c/r_s \leq 1.14$, implying that the number of sensors it needs over optimal decreases in this range. At $r_c = r_s$, it needs 44% more nodes than the optimal. When $r_c/r_s < 1$, however, the number of sensors it needs over the optimal, starts to increase exponentially. The number of sensors needed by other regular patterns in this range of r_c/r_s, is only worse. The implication is that when $r_c/r_s < 1$, using the strip-based pattern over other regular patterns of deployment can result in significant saving in the number of sensors needed.

7. CONCLUSION

In this paper, we addressed the problem of determining an optimal deployment pattern that achieves both coverage and k-connectivity. We proposed a strip-based deployment pattern to achieve coverage and 2-connectivity, and proved its optimality. We also proved the optimality of a previously proposed strip-based deployment pattern to achieve coverage and 1-connectivity. Finally, we established the efficiency of popular regular patterns of deployment, thus enabling a deployer make a more informed decision.

Several problems still remain open in this space, though. The problem of determining an optimal deployment pattern that achieves ℓ-coverage and k-connectivity for general values of ℓ and k is still open. Also, the problem of determining optimal deployment patterns that use statistical models of sensing and communication ranges to make probabilistic guarantees on coverage and connectivity, is yet to be addressed. We plan to address these open problems in our future work.

8. ACKNOWLEDGMENTS

We thank our shepherd Doug Blough and anonymous referees whose comments helped us improve the presentation of this paper. We also thank József Balogh from the department of Mathematics at UIUC for sharing his insights on this problem. Our research is partially supported by NSF grants ACI-0329155, CCF-0546668, and by NSFC grant 10571151. This research does not reflect the views of NSF or NSFC.

9. REFERENCES

[1] A. Arora and et. al. ExScal: Elements of an Extreme Scale Wireless Sensor Network. In *11th IEEE International Conference on Real-Time Computing Systems and Applications (IEEE RTCSA),* Hong Kong, 2005.

[2] S. Bapat, V. Kulathumani, and A. Arora. Analyzing the Yield of ExScal, a Large Scale Wireless Sensor Network Experiment. In *13th IEEE International Conference on Network Protocols (ICNP),* Boston, MA, 2005.

[3] Q. Cao, T. Yan, J. A. Stankovic, and T. F. Abdelzaher. Analysis of Target Detection Performance for Wireless Sensor Networks. In *International Conference on Distributed Computing in Sensor Networks (DCOSS),* 2005.

[4] F. S. Hillier and G. J. Lieberman. *Introduction to Operations Research.* McGraw-Hill, 2002.

[5] R.Iyengar, K. Kar and S. Banerjee. Low-coordination Topologies for Redundancy in Sensor Networks. In *the Sixth ACM Annual International Symposium on Mobile Ad-Hoc Networking and Computing (MobiHoc),* pages 332-342, Urbana-Champaign, IL, 2005.

[6] R. Kershner. The Number of Circles Covering a Set. *American Journal of Mathematics,* 61:665-671, 1939.

[7] Y.-C. Wang, C.-C. Hu, and Y.-C. Tseng. Efficient Deployment Algorithms for Ensuring Coverage and Connectivity of Wireless Sensor Networks. In *Wireless International Conference (WICON),* Budapest, Hungary, 2005.

[8] G. Xing, X. Wang, Y. Zhang, C. Lu, R. Pless, and C. Gill. Integrated Coverage and Connectivity Configuration in Wireless Sensor Networks. *ACM Transactions on Sensor Networks,* 1(1):36-72, 2005.

[9] H. Zhang and J. Hou. Maintaining Sensing Coverage and Connectivity in Large Sensor Networks. In *NSF International Workshop on Theoretical and Algorithmic Aspects of Sensor, Ad Hoc Wirelsss, and Peer-to-Peer Networks,* 2004.

[10] J. Zhao and R. Govindan. Understanding Packet Delivery Performance in Dense Wireless Sensor Networks. In *ACM Conference on Ebmedded Networked Sensor Systems (SenSys),* pages 1-13, Los Angeles, CA, 2003.

[11] G. Zhou, T. He, S. Krishnamurthy, and J. A. Stankovic. Impact of Radio Irregularity on Wireless Sensor Networks. In *ACM MobiSys,* pages 125-138, Boston, MA, 2004.

10. APPENDIX A

In this appendix, we make extensive use of Definitions 2.8 and 2.9. We first develop a series of lemmas (Lemma 10.1 through Lemma 10.5). For these lemmas, the following fact on $|\Psi_{k,n}|$, which follows from the definition of Ψ (see Definition 2.9), is extensively used in the proofs that are omitted in this paper.

$$|\Psi_{k,n}| = \frac{1}{2}r_s^2\left(n\sin\varphi + (k-n)\sin\frac{2\pi - n\varphi}{k-n}\right).$$

LEMMA 10.1. *Let $e_i, 1 \le i \le k$, be the edges of a $\Phi_{k,n}$ such that $\forall i : 1 \le i \le n : |e_i| \ge \ell$, where ℓ is as defined in Definition 2.5. Also, let $\Phi'_{k,n}$ be a k-sided polygon inscribed in D_{r_s} such that it has n sides, each with length $(e_1+\cdots+e_n)/n$, with remaining sides having equal length (potentially different from $(e_1 + \ldots + e_n)/n$). Finally, let $|\Phi'_{k,n}|$ be the area of polygon $\Phi'_{k,n}$. Then, $|\Phi_{k,n}| \le |\Phi'_{k,n}|$.*

LEMMA 10.2. *If $k \ge 6$, then $|\Phi_{k,n}| \le |\Psi_{k,n}|$.*

LEMMA 10.3. *If $k \ge 6$ and $n_1 \ge n_2$, then $|\Psi_{k,n_1}| \le |\Psi_{k,n_2}|$.*

LEMMA 10.4. *If $k_1 \le k_2$, then $|\Psi_{k_1,n}| \le |\Psi_{k_2,n}|$.*

LEMMA 10.5. *If $n_1 \ge 1$ and $k_1 - n_1 \ge 5$, then $|\Psi_{k_1,n_1}| - |\Psi_{k_1-1,n_1}| \le |\Psi_{6,1}| - |\Psi_{5,1}|$.*

We now prove Lemma 4.2.

PROOF. In our proof, The basic idea we use in proving Lemma 4.2 is a series of ***allowed*** transformations that change Φ_{k_i,n_i} $(1 \le i \le m)$ into $\Psi_{6,2}$. We consider a transformation ***allowed*** if and only if it changes some Φ_{k_i,n_i}, and its result still satisfies the three conditions, but doesn't reduce the value of $\sum_{i=1}^{m}|\Phi_{k_i,n_i}|$.

By Lemma 10.1, we may assume that for a $\Phi_{k,n}$, n edges of length at least ℓ are equal to each other in length, as are the other $(k-n)$ edges. By Lemma 10.2, we may further assume that a $\Phi_{k,n}$ is a $\Psi_{k,n}$ for $k \ge 6$. Lemma 10.3 through 10.5 show the relationship between areas of the chord polygons used in transformation.

When $\pi/3 < \varphi < \pi$, we have $r_s < \ell < 2r_s$, which we can divide into three subintervals $r_s < \ell \le \sqrt{2}r_s$, $\sqrt{2}r_s < l \le \sqrt{3}r_s$, and $\sqrt{3}r_s < l < 2r_s$.

We first prove the lemma in the subinterval $r_s < \ell \le \sqrt{2}r_s$ so that $\pi/3 < \varphi \le \pi/2$. For $k \le 3$, no $\Phi_{k,n}$ exists for this range of φ. Therefore, we only consider $k \ge 4$. For $k = 4$, n has to be 4 so that we only have $\Phi_{4,4}$, i.e., $\Psi_{4,4}$.

We divide our proof in six steps.

Step 1. If $\nexists i : 1 \le i \le m$ such that $k_i > 6$, then we may transform each Φ_{k_i,n_i} for $n_i > 1$ into Ψ_{6,n_i} and then transform Ψ_{6,n_i} into $\Psi_{6,2}$. By Lemma 10.3 and Lemma 10.4, it can be verified that this transformation is allowed. For $\Phi_{5,1}$, notice $2\pi/5 < \varphi \le \pi/2$, transform it to $\Psi_{6,2}$. This transformation is allowed and then Lemma 4.2 is proved. Hence, we may assume that $\exists i$ such that $k_i > 6$.

Step 2. In this subinterval $r_s < \ell \le \sqrt{2}r_s$, no $\Psi_{k_i,1}$ exists when $k_i < 5$. If $\exists j$ such that $k_j > 6$ and $k_j - n_j > 4$, then we may transform $\Phi_{5,1}$ into $\Psi_{6,1}$, and at the same time transform Ψ_{k_j,n_j} into Ψ_{k_j-1,n_j}. By Lemma 10.5, this transform is allowed. If such a j does not exist, we only have $\Psi_{7,3}, \Psi_{7,4}, \Psi_{7,5}, \Psi_{8,4}, \Psi_{8,5}$ and $\Psi_{9,5}$ for $k_i > 6$. It can be verified that, among all the decreases in area that result from transforming these six Ψ_{k_i,n_i} into Ψ_{k_i-1,n_i}, the biggest occurs when transforming $\Psi_{7,3}$ into $\Psi_{6,3}$. So we only need to prove that the transformation which transforms $\Phi_{5,1}$ into $\Psi_{6,1}$ and at the same time transforms $\Psi_{7,3}$ into $\Psi_{6,3}$ is allowed. In fact, the transformation which transforms $\Phi_{5,1}$ into $\Psi_{6,1}$ will increase the area of the polygon by at least

$$\frac{1}{2}r_s^2\left(5\sin\frac{3\pi}{10} - 4\sin\frac{3\pi}{8}\right) = 0.1748\cdots r_s^2,$$

and the transformation that transforms $\Psi_{7,3}$ into $\Psi_{6,3}$ will decrease the area by at most

$$\frac{1}{2}r_s^2\left(4\sin\frac{\pi}{4} - 3\sin\frac{\pi}{3}\right) = 0.1152\cdots r_s^2.$$

Hence, the above transformation is allowed. Therefore, we may assume that $n_i \ne 1$ for $k_i < 6$. We may further assume that there must exist $\Psi_{k_i,1}$ or $\Psi_{k_i,2}$ for $k_i > 5$. Otherwise, we can transform Ψ_{k_i,n_i} into $\Psi_{k_i,2}$ for each $k_i > 5$, and by Lemma 10.3, this transformation is allowed.

Step 3. Let $\Psi = \{\Psi_{k_i,n_i} : k_i > 6\}$ and $\Psi' = \{\Phi_{k_i,n_i} : k_i < 6\}$. By Step 2 above, we only need to consider $\Phi_{4,4}$ and $\Phi_{5,n}$ for $1 < n \le 5$ in Ψ'.

We define a relation (or multivalued mapping) R from Ψ to Ψ' as follows such that for any pair $\Psi_{k_i,n_i}, \Psi_{k_j,n_j} \in \Psi$ $(i \ne j)$, either $R(\Psi_{k_i,n_i}) = R(\Psi_{k_j,n_j})$ or $R(\Psi_{k_i,n_i}) \cap R(\Psi_{k_j,n_j}) = \emptyset$.

Let $\Psi_{k_{i_1},n_{i_1}} \in \Psi$. We consider the odd and even values of k_{i_1} separately.

Case 1. k_{i_1} is odd.

(1) If $\exists \Phi_{5,n} \in \Psi'$, then one $\Phi_{5,n}$ and $\frac{k_{i_1}-7}{2}$ $\Phi_{4,4}$ are taken from Ψ' as the value of $R(\Psi_{k_{i_1},n_{i_1}})$. When there are not enough $\Phi_{4,4}$, two $\Phi_{5,n}$ can be used instead.

(2) If $\nexists \Phi_{5,n} \in \Psi'$ and $\nexists \Psi_{k_{i_2},n_{i_2}} \in \Psi$ with $i_2 \neq i_1$ for odd k_{i_2}, then $\frac{k_{i_1}-6+1}{2}$ $\Phi_{4,4}$ are taken from Ψ' as the value for $R(\Psi_{k_{i_1},n_{i_1}})$.

(3) If $\nexists \Phi_{5,n} \in \Psi'$ and $\nexists \Psi_{k_{i_2},n_{i_2}} \in \Psi$ with $i_2 \neq i_1$ for odd k_{i_2}, then $\frac{k_{i_1}+k_{i_2}-6}{2}$ $\Phi_{4,4}$ are taken from Ψ' as the value for both $R(\Psi_{k_{i_1},n_{i_1}})$ and $R(\Psi_{k_{i_2},n_{i_2}})$.

Case 2. k_{i_1} is even.

Then, the value for $R(\Psi_{k_{i_1},n_{i_1}})$ is $\frac{k_{i_1}-6}{2}$ $\Phi_{4,4}$ in Ψ' . When there are not enough $\Phi_{4,4}$, two $\Phi_{5,n}$ can be used instead.

For a given $\Psi_{k,n} \in \Psi$, if $\exists R(\Psi_{k,n})$, then we define

$$R^{-1}R(\Psi_{k,n}) = \{\Psi_{k_i,n_i} \in \Psi : R(\Psi_{k,n}) = R(\Psi_{k_i,n_i})\}.$$

Let Ψ be $\Psi \setminus R^{-1}R(\Psi_{k_{i_1},n_{i_1}})$. Then we take a $\Psi_{k_i,n_i} \in \Psi$, and then repeat above procedure to define $R(\Psi_{k_i,n_i}) \subseteq \Psi' \setminus R(\Psi_{k_{i_1},n_{i_1}})$. After finite steps, the relation R will be completely specified.

For a $\Phi_{k_i,n_i} \in \Psi'$, we define

$$R^{-1}(\Phi_{k_i,n_i}) = \{\Psi_{k_j,n_j} \in \Psi : \Phi_{k_i,n_i} \in R(\Psi_{k_j,n_j})\}.$$

From condition (1) in the lemma, there may exist some $\Phi_{k_i,n_i} \in \Psi'$ such that $R^{-1}(\Phi_{k_i,n_i}) = \emptyset$. For all $\Phi_{k_i,n_i} \in \Psi'$ with $R^{-1}(\Phi_{k_i,n_i}) = \emptyset$, we transform it to $\Psi_{6,2}$. It can be verified that this transformation is allowed. Hence, we may assume that for any $\Phi_{k_i,n_i} \in \Psi'$, $R^{-1}(\Phi_{k_i,n_i}) \neq \emptyset$.

Step 4. Without loss of generality, we may assume that $R^{-1}(\Phi_{4,4}) = \Psi_{8,1}$ or that $R^{-1}(\Phi_{4,4})$ consists of two $\Psi_{7,1}$. (For, otherwise, there must be some $\Phi_{k_i,n_i} \in \Psi'$ such that $R^{-1}(\Phi_{k_i,n_i}) = R^{-1}(\Phi_{4,4})$, and we can transform all the other Φ_{k_i,n_i} into $\Psi_{6,2}$, and at the same time transform $R^{-1}(\Phi_{4,4})$ into $\Psi_{8,1}$ or two $\Psi_{7,1}$. It can be also verified that the above transformation is allowed.)

If $R^{-1}(\Phi_{4,4}) = \Psi_{8,1}$, then we transform $\Phi_{4,4}$ and $\Psi_{8,1}$ into two $\Psi_{6,2}$. Since changing a $\Phi_{4,4}$ into a $\Psi_{6,2}$ will increase the area of the polygon by

$$\frac{1}{2}r_s^2\left(4\sin\frac{\pi}{4} - 2\sin\frac{\pi}{2}\right) = 0.4142\cdots r_s^2,$$

while transforming $\Psi_{8,1}$ into $\Psi_{6,2}$ will decrease the area of the polygon by at most

$$\frac{1}{2}r_s^2\left(7\sin\frac{3\pi}{14} - 4\sin\frac{4\pi}{4} - \sin\frac{\pi}{2}\right) = 0.2282\cdots r_s^2.$$

Hence, this transformation is allowed.

If $R^{-1}(\Phi_{4,4})$ consists of two $\Psi_{7,1}$, we transform the $\Phi_{4,4}$ and the two $\Psi_{7,1}$ into three $\Psi_{6,2}$. Since changing two $\Psi_{7,1}$ into two $\Psi_{6,2}$ will decrease the area of the polygon by at most

$$r_s^2\left(2sin\frac{\pi}{4} - sin\frac{\pi}{2}\right) = 0.4142\cdots r_s^2.$$

Hence, this transformation is also allowed.

Step 5. For $\Phi_{5,j} \in \Psi'(j = 2, 3, 4)$, using a similar argument as in step 4, we may assume that $R^{-1}(\Phi_{5,j}) = \Psi_{7,1}$. We transform $\Phi_{5,j}$ and $\Psi_{7,1}$ into two $\Psi_{6,2}$. Since changing a $\Phi_{5,j}$ $(j = 2, 3, 4)$ into a $\Psi_{6,2}$ will increase the area of the polygon by at least

$$\frac{1}{2}r_s^2\left(4\sin\frac{3\pi}{10} - 3\sin\frac{2\pi}{5}\right) = 0.1914\cdots r_s^2,$$

for $j = 2, 3, 4$, while changing $\Psi_{7,1}$ into $\Psi_{6,2}$ will decrease the area by at most

$$\frac{1}{2}r_s^2\left(6\sin\frac{5\pi}{18} - 5\sin\frac{\pi}{6}\right) = 0.1330\cdots r_s^2.$$

Hence, this transformation is also allowed.

Step 6. We may assume that $R^{-1}(\Phi_{5,5}) = \Psi_{7,1}$. We transform $\Phi_{5,5}$ and $\Psi_{7,1}$ into two $\Psi_{6,2}$. When transforming a $\Phi_{5,5}$ into a $\Psi_{6,2}$ will increase the area of the polygon by

$$\frac{1}{2}r_s^2\left(2\sin\frac{2\pi}{5} + 4\sin\frac{3\pi}{10} - 5\sin\frac{2\pi}{5}\right) = 0.1914\cdots r_s^2,$$

while transforming $\Psi_{7,1}$ into $\Psi_{6,2}$ will decrease the area by at most

$$\frac{1}{2}r_s^2\left(\sin\frac{2\pi}{5} + 6\sin\frac{4\pi}{15} - 2\sin\frac{2\pi}{5} - 4\sin\frac{3\pi}{10}\right) = 0.1358\cdots r_s^2.$$

Hence, this transformation is allowed.

After these 6 steps, we are left with only $\Psi_{6,2}$, and thus the lemma is proved for $r_s < \ell \leq \sqrt{2}r_s$.

When $\sqrt{2}r_s < l \leq \sqrt{3}r_s$, $\Phi_{3,3}, \Phi_{4,1}, \Phi_{4,2}, \Phi_{4,3}$ become possible. When $\sqrt{3}r_s < l < 2r_s$, $\Phi_{3,1}, \Phi_{3,2}$ also become possible. The proof for these two subintervals can be carried out along the similar lines as done for the first subinterval. □

11. APPENDIX B

THEOREM 11.1. (Theorem in [6]) *Let M denote a bounded plane point set and let $N(\epsilon)$ be the minimum number of circles of radius ϵ which can cover M. Then*

$$\lim_{\epsilon\to 0} \pi\epsilon^2 N(\epsilon) = (2\sqrt{3}/9)\ meas\ \bar{M}, \tag{36}$$

where $\bar{M}$ denotes the closure of M.

LEMMA 11.1. (Lemma 1 in [6]) *Let Γ denote a bounded plane network consisting of a finite number of finite polygons. Suppose that each vertex of Γ is on at least three edges. Then the average number of sides of the polygons of Γ is < 6.*

LEMMA 11.2. (Lemma 2 in [6]) *Let σ be a fixed circle and let A_k denote the area of a regular polygon of k sides inscribed in σ. Then for $k \geq 3$,*

$$0 < A_{k+1} - A_k < A_k - A_{k-1}. \tag{37}$$

LEMMA 11.3. (Lemma 3 in [6]) *With the notations of above lemma, and $k > j \geq 3$,*

$$(k-j)(A_k - A_{k-1}) \leq A_k - A_j \leq (k-j)(A_{j+1} - A_j). \tag{38}$$

LEMMA 11.4. (Lemma 4 in [6]) *Let Γ denote a bounded plan network consisting of F finite polygons. Suppose that each vertex of Γ is on at least three edges. Suppose, finally, that each polygon of Γ can be covered by a circle σ of fixed radius r. Then the total area of Γ is $< FA_6$, where $A_6 = (3\sqrt{3}/2)r^2$ is the area of a regular hexagon inscribed in σ.*

LEMMA 11.5. (Lemma 5 in [6]) *Let ρ denote a rectangle in the plane with area R. Let $N(\epsilon)$ denote the minimum number of circles of radius ϵ which can cover ρ. Then*

$$\pi\epsilon^2 N(\epsilon) > (2\pi\sqrt{3}/9)(R - 2\pi\epsilon^2). \tag{39}$$

LEMMA 11.6. (Lemma 6 in [6]) *Let ρ denote a rectangle in the plane with area R and perimeter p. Let $N(\epsilon)$ denote the minimum number of circles of radius ϵ which cover ρ. Then*

$$\pi\epsilon^2 N(\epsilon) < (2\pi\sqrt{3}/9)(R + 2\pi\epsilon + 16\epsilon^2). \tag{40}$$